



**HAL**  
open science

## **Partitioning of oblique convergence in the Northern Andes subduction zone: Migration history and the present-day boundary of the North Andean Sliver in Ecuador**

Alexandra Alvarado Cevallos Alvarado, L. Audin, J.M. Nocquet, Etienne Jaillard, P. Mothes, P. Jarrin, M. Segovia, Frédérique Rolandone, D. Cisneros

### ► To cite this version:

Alexandra Alvarado Cevallos Alvarado, L. Audin, J.M. Nocquet, Etienne Jaillard, P. Mothes, et al.. Partitioning of oblique convergence in the Northern Andes subduction zone: Migration history and the present-day boundary of the North Andean Sliver in Ecuador. *Tectonics*, 2016, 35 (5), pp.1048-1065. 10.1002/2016TC004117 . hal-01402144

**HAL Id: hal-01402144**

**<https://hal.science/hal-01402144>**

Submitted on 18 May 2021

**HAL** is a multi-disciplinary open access archive for the deposit and dissemination of scientific research documents, whether they are published or not. The documents may come from teaching and research institutions in France or abroad, or from public or private research centers.

L'archive ouverte pluridisciplinaire **HAL**, est destinée au dépôt et à la diffusion de documents scientifiques de niveau recherche, publiés ou non, émanant des établissements d'enseignement et de recherche français ou étrangers, des laboratoires publics ou privés.

## RESEARCH ARTICLE

10.1002/2016TC004117

## Key Points:

- New tectonic and geodetic data unambiguously define the present-day boundary of the NAS in Ecuador
- The present-day major boundary does not follow old sutures like the Dolores Guayaquil Megashear
- Cenozoic partitioning of the deformation developed by successive narrowing restraining bends

## Correspondence to:

L. Audin,  
laurence.audin@ird.fr

## Citation:

Alvarado, A., L. Audin, J. M. Nocquet, E. Jaillard, P. Mothes, P. Jarrin, M. Segovia, F. Rolandone, and D. Cisneros (2016), Partitioning of oblique convergence in the Northern Andes subduction zone: Migration history and the present-day boundary of the North Andean Sliver in Ecuador, *Tectonics*, 35, 1048–1065, doi:10.1002/2016TC004117.

Received 15 JAN 2016

Accepted 8 APR 2016

Accepted article online 13 APR 2016

Published online 3 MAY 2016

## Partitioning of oblique convergence in the Northern Andes subduction zone: Migration history and the present-day boundary of the North Andean Sliver in Ecuador

A Alvarado<sup>1,2</sup>, L Audin<sup>2</sup>, J. M Nocquet<sup>3</sup>, E Jaillard<sup>2</sup>, P Mothes<sup>1</sup>, P Jarrin<sup>1</sup>, M. Segovia<sup>1</sup>, F Rolandone<sup>4</sup>, and D Cisneros<sup>5</sup>

<sup>1</sup>Instituto Geofísico, Escuela Politécnica Nacional, Quito, Ecuador, <sup>2</sup>Institut des Sciences de la Terre, IRD: UR219, Université Joseph Fourier–Grenoble I–INSU–OSUG, Grenoble, France, <sup>3</sup>Géoazur, CNRS, Université de Nice Sophia–Antipolis, IRD, Observatoire de la Côte d’Azur, Valbonne, France, <sup>4</sup>Sorbonne Universités, UPMC Université Paris 06, CNRS, Institut des Sciences de la Terre de Paris, Paris, France, <sup>5</sup>Instituto Geográfico Militar, Quito, Ecuador

**Abstract** Along the Ecuadorian margin, oblique subduction induces deformation of the overriding continental plate. For the last 15 Ma, both exhumation and tectonic history of Ecuador suggest that the northeastward motion of the North Andean Sliver (NAS) was accompanied by an eastward migration of its eastern boundary and successive progressively narrowing restraining bends. Here we present geologic data, earthquake epicenters, focal mechanisms, GPS results, and a revised active fault map consistent with this new kinematic model. All data sets concur to demonstrate that active continental deformation is presently localized along a single major fault system, connecting fault segments from the Gulf of Guayaquil to the eastern Andean Cordillera. Although secondary faults are recognized within the Cordillera, they accommodate a negligible fraction of relative motion compared to the main fault system. The eastern limit is then concentrated rather than distributed as first proposed, marking a sharp boundary between the NAS, the Inca sliver, and the Subandean domain overthrusting the South American craton. The NAS limit follows a northeast striking right-lateral transpressional strike-slip system from the Gulf of Guayaquil (Isla Puná) to the Andean Cordillera and with the north-south striking transpressive faults along the eastern Andes. Eastward migration of the restraining belt since the Pliocene, abandonment of the sutures and reactivation of north-south striking ancient fault zones lead to the final development of a major tectonic boundary south and east of the NAS, favoring its extrusion as a continental sliver, accommodating the oblique convergence of the Nazca oceanic plate toward South America.

### 1. Introduction

Geodynamic evolution of the Northern Andes departs from the classical Andean subduction type [Uyeda and Kanamori, 1979; Lallemand, 1999]. Along the northwestern margin of South America, subduction of the oceanic Farallón plate occurs since at least 190 Ma and interacted with the progressive development of the Caribbean domain to the North. This plate interaction led to large-scale lithospheric deformation of northern South America involving several individualized continental blocks (Figure 1) [Audemard and Audemard, 2002; Pindell and Kennan, 2009]. Furthermore, between 75 and 58 Ma, oceanic terranes have been accreted to the Ecuadorian continental margin through successive episodes [Reynaud *et al.*, 1999; Spikings *et al.*, 2001; Jaillard *et al.*, 2004, 2008, 2009], before the main orogeny phase started 23 Ma ago [Hey, 1977; Audemard and Audemard, 2002]. In the latest stage of the Northern Andes evolution, an upper plate “sliver” in Ecuador and Colombia, trapped between the trench and the South American craton (i.e., the Guyanese Shield) is “escaping” NE-ward since the Mio-Pliocene [Pennington, 1981; Costa *et al.*, 2009; Egbue and Kellogg, 2010; Nocquet *et al.*, 2014].

Since early observations by Fitch [1972], many studies have recognized that the overriding plate in subduction zones experiences intense deformation, leading to the formation of partly detached on board continental domains, wedged between the trench and the stable part of the upper plate. The words “Forearc slivers” [Beck, 1991; McCaffrey, 1992], “blocks” [Pennington, 1981], “microplate” [Brooks *et al.*, 2003], and “continental slivers” [Nocquet *et al.*, 2014] have interchangeably been used by the authors depending on the local context. In this paper, we choose to use the term “North Andean Sliver” (NAS) for the following reasons: (1) the mobile domain encompasses not only the fore-arc domain but sometimes also comprises part of the arc and back-arc domains; (2) we believe that blocks or microplate refer to a domain without any significant internal

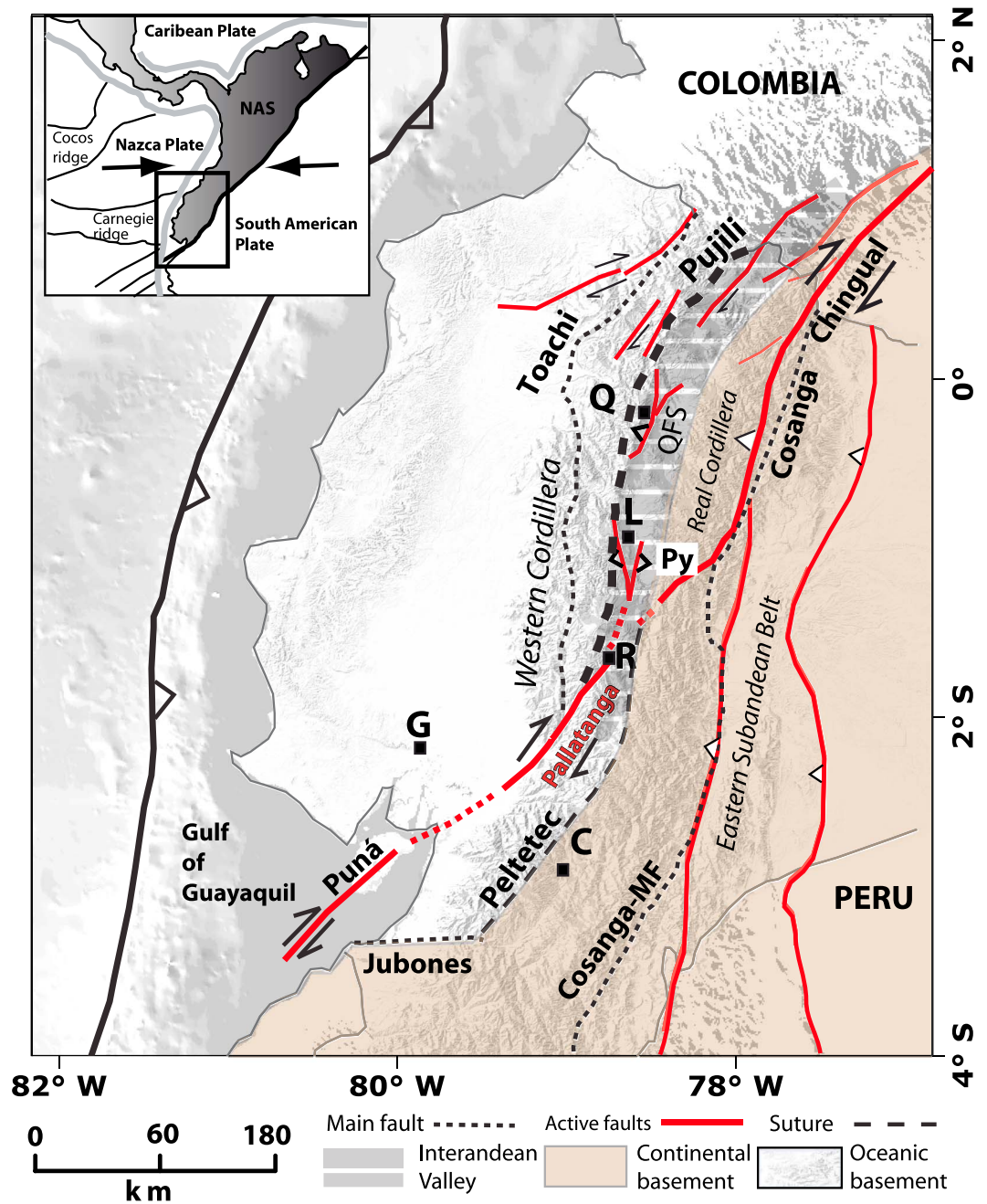


**Figure 1.** New active tectonic map of Ecuador. Major fault segments and their kinematics are reported in continuous red lines. The principal sutures zones are drawn in black dotted lines [after Zamora and Litherland, 1993; Aspden and Litherland, 1992; Hughes and Pilatasig, 2002; Jaillard et al., 2009]. The regional geodynamic setting is represented in inset [after Audemard and Audemard, 2002]. Active volcanic centers are also reported on the topographic map. North Andean Sliver: NAS; Cosanga-Méndez Fault, as defined by Aspden and Litherland [1992]: Cosanga-MF; Peltetec suture: Peltetec; Pujilí Melange Suture: Pujili; Jubones Fault: Jubones; Toachi shear zone: Toachi; Pisayambo zone: Py. QFS: Quito active Fault System. Cities: Quito: Q; Latacunga: L; Cuenca: C; Riobamba: R; Guayaquil: G.

deformation, which is usually not the case [e.g., Gordon, 1995]. The existence of internal deformation within the NAS has further been demonstrated by Alvarado et al. [2014] for the Quito Fault System and by Lavenu et al. [1995] for the Interandean Valley, precluding the use of “block” or microplate (3) the domain showing coherent motion displays a large length/width ratio (here extending about 2200 km from the Gulf of Guayaquil to Venezuela with a width <450 km and is small compared to the size of the South America plate).

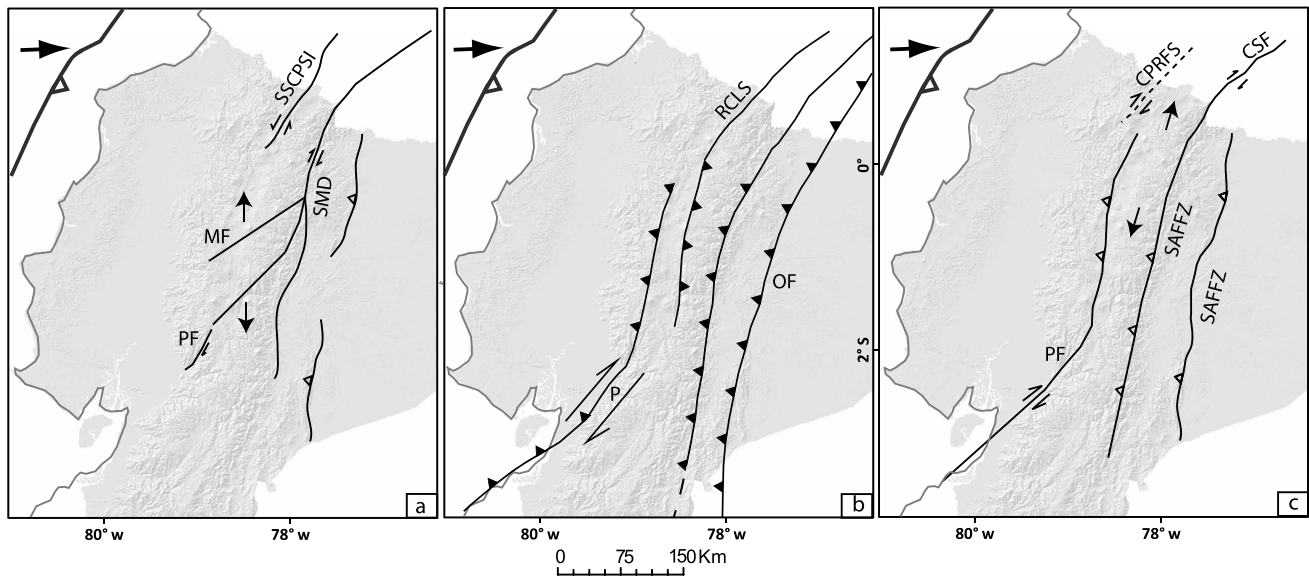


**Figure 2.** Previously published tectonic models: (a) After *Soulas et al.* [1991], implicating the following fault systems: “Sistema Senestral Cauca-Patía-San Isidro” SSCPSI, “Sistema Mayor Dextral” SMD, Pallatanga fault PF, Machachi fault MF. (b) After *White et al.* [2003], implicating the following fault systems: Pallatanga fault P, Río Chingual-La Sofía RCLS, Oriente Fault OF. (c) After *Ego et al.* [1996], implicating the following fault systems: “Cauca Patía and Romeral Fault System” CPRFS and “Pallatanga Fault” PF and the Cretaceous suture zone, “Sub Andean Front Fault Zone” SAFFZ and “Chingual–La Sofía fault” CSF.

Several models have described in general terms the escape of the NAS and proposed the driving mechanisms, but none have discussed its geographical boundaries or evolution through time. So far, studies of the NAS fall into two different conceptual categories. On the one hand, some models propose the distribution of the deformation as taking place along several fault strands equally active, but localizing the deformation at the scale of the lithosphere (Figure 2a) [*Soulas et al.*, 1991; *Egbue and Kellogg*, 2010]. Consequently, the NAS would be divided in a succession of N-S domains (Figure 2b) [*White et al.*, 2003]. Conversely, other models consider the eastern limit of the NAS as a restraining bend located along the Interandean Depression (Figure 2c) [*Ego et al.*, 1996].

Here we present an integrated view of the tectonic evolution of the Ecuadorian Andes over the last 15 Ma, based on all available geodynamic data. The main goals of this review paper are the following: (1) to address the Neogene geologic and tectonic history of a key part of the Northern Andes through a critical review of previously published works and (2) to provide new, high-quality GPS and structural data in order to unambiguously define the present-day eastern limit of the NAS. Based on these results, we propose an evolution model showing how oblique plate convergence has been accommodated within the South American continent in Ecuador at least since the Miocene. This model is used to discuss the role of tectonic heritage of continental sutures.

### 1.1. Sutures and Inherited Tectonic Structures

In major active mountain ranges, suture zones are considered as fundamental inherited lithospheric structures. In Tibet, for example, sutures usually indicate the contact of margin rocks with exotic terrains and control the further evolution of the orogeny and the location of deformation [*Guillot and Replumaz*, 2013]. Sutures can thus be reactivated or abandoned through time at the favor of compatible convergence directions, especially as strike-slip fault systems. For instance, in Tibet, it has been proposed that boundary forces resulted in stresses sufficient to reactivate weakly welded sutures [*Tapponnier et al.*, 2001]. Similarly to Tibet, rocks on either side of inherited suture zones of Ecuador belong to fundamentally different tectonic or metamorphic regions: oceanic plateaus and island arcs dominate to the West or NW, and the Brazilian shield is found to the East and SE (Figure 1).

Ecuador is subdivided into tectonostratigraphic zones that extend parallel to the length of the Northern Andean range (Figure 1). The Coastal region and the Western Cordillera comprise the various accreted oceanic terranes, separated from each other by Cretaceous fault systems (Figure 1) [*Luzieux et al.*, 2006; *Jaillard*

*et al.*, 2009]. The Interandean Valley comprises the Plio-Quaternary Volcanic zone, the main volcanic centers being distributed in the Western and Real Cordilleras [Hall *et al.*, 2008]. Their products overlay part of the accreted terrains and mask the eastern contact with the continental crystalline rocks to the east (Figure 1) [Aspden and Litherland, 1992]. Although the eastern Cordillera Real and Subandean ranges are covered by dense tropical vegetation, most of these regions exhibit metamorphic rocks and sedimentary cover [Zamora and Litherland, 1993]. The review paper by Jaillard *et al.* [2009] suggests that the lateral escape of the NAS might have been active since the Late Cretaceous and has been accommodated along several suture zones [Pennington, 1981; Kellogg and Vega, 1995; Egbue and Kellogg, 2010]. We compiled the information on a comprehensive map of the sutures and limits of the oceanic accreted terranes for all Ecuador (Figure 1). It shows that the terrain slivers extend laterally for several hundreds of kilometers in a roughly north-northeast direction along the northern Andes (Figure 1). These are only a few tens of kilometers wide and are separated by deep crustal suture zones, sometimes seismically reactivated at depth [Guillier *et al.*, 2001].

Two different kinds of suture zones and fault systems summarized in this compilation have been previously identified (Figure 1) [Feininger, 1987; Lebras *et al.*, 1987; Aguirre, 1992; Van Thournout *et al.*, 1992; Reynaud *et al.*, 1999; Hughes and Pilatasig, 2002; Kerr *et al.*, 2002; Mamberti *et al.*, 2003; Jaillard *et al.*, 2009]. The first one illustrates the major phases of deformation recorded by the continental metamorphic domains, while the second marks the geographic eastern limit of the accreted oceanic terranes (Figures 3 and 4). Southern Ecuador marks the transition from the Central Andes of Peru to the Northern Andes of Ecuador and Colombia [Zamora and Litherland, 1993]. In Figure 3, our new geologic map of the Pallatanga region, in SW Ecuador, reflects the structural evolution of this area during the Cretaceous. While most inherited and inactive major fault systems strike parallel to the orogen and are roughly perpendicular to the direction of convergence (Figure 3), there are several deviations from this system, including transpressional shear zones that bound the Northern Andean Sliver. Strong structuration of the topography and geological formations by east striking fault systems, northeast striking fault systems, and sutures, are seen, for example, in the Jubones fault zone (Figures 1 and 3). The Cosanga and Méndez Faults are part of the same ancient tectonic system (Figure 4). First active during the Jurassic, the Cosanga-Méndez Fault System marks the limit between the metamorphic rocks of the Cordillera Real and nondeformed domains of the Subandean zone [Aspden and Litherland, 1992]. The Pelitetec Suture zone marks the boundary between the pre-Jurassic continental crystalline rocks and Jurassic island arc rocks, as described by Aspden and Litherland [1992] near Riobamba (Figure 4). To the South, the Jubones suture zone marks another limit between continental and oceanic domains and corresponds to the southern extension of the Pelitetec Suture zone. The Pujilí Melange and its suture zone, first defined by Hughes and Pilatasig [2002], show a dextral strike-slip displacement that carried the oceanic terranes, forming the basement of the Western Cordillera (Figure 4). Rather narrow, this suture zone presents highly deformed outcrops of mainly ophiolitic rocks [Hughes and Pilatasig, 2002]. The last accretion is dated from the Paleocene when the Piñón terrain was accreted onto the continent [Jaillard *et al.*, 2009]. The eastern limit of this terrain approximately coincides with a tectonic boundary, the Toachi shear zone [Hughes and Pilatasig, 2002; Jaillard *et al.*, 2009] (Figure 4). Note that some authors proposed the above listed tectonic sutures to be nowadays reactivated [Guillier *et al.*, 2001].

## 1.2. Kinematic Evolution of Large-Scale Deformation in Ecuador Since the Late Cretaceous and Its Paleogeographic Interpretation

The history of the large-scale deformation in Ecuador involves a succession of discrete and intense tectonic events rather than deformation continuous through time. Accretion of oceanic terranes to the Ecuadorian continental margin occurred between 75 and 58 Ma [Reynaud *et al.*, 1999; Spikings *et al.*, 2001; Jaillard *et al.*, 2004, 2008, 2009]. Since then, NE-ward oceanic convergence led to the activation of the former sutures bounding the oceanic terranes as dextral strike-slip faults and flower structures [Jaillard *et al.*, 2004, 2009; Amortegui *et al.*, 2011], according to a sequence of events. During the Cretaceous-Eocene time span, a series of pull-apart basins formed in the Western Cordillera in relation to strike-slip movement along the suture zones [Toro, 2007]. The formation of these basins concluded in the Eocene [Toro, 2007] and was coeval with the exhumation of the whole Western Cordillera [Spikings *et al.*, 2010; Hoorn *et al.*, 2010] (Figure 3). Here N-S striking flower structures crosscut Oligocene volcanic deposits, showing that they were active until late Oligocene to Miocene times (Figure 3). These transpressional structures were subsequently cut and offset by NE trending dextral faults, whose activity can be dated as late Miocene, since they crosscut the Oligocene volcanic pile (Figure 3). However, these faults were not reactivated in the Quaternary and do

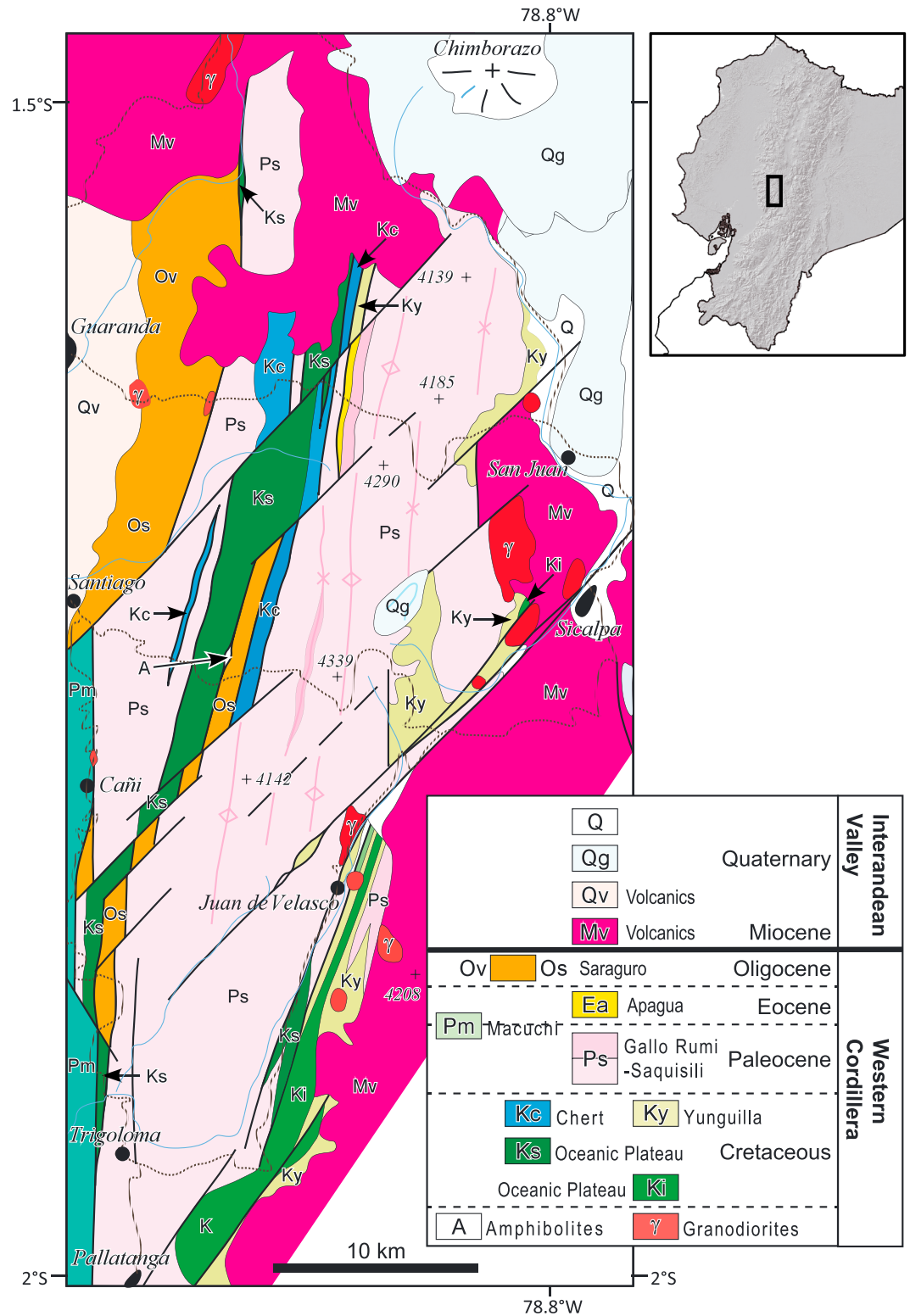


**Figure 3.** New geological map of the southern Western Cordillera, in Pallatanga region (1°30'–2°S). Note the systematic right lateral NE offset, dated as late Miocene and the systematic offset of older (late Oligocene to Miocene) NS sutures and terranes north of Juan de Velasco village. These NE faults do not affect the Quaternary to recent volcanic outcrops in the Interandean Valley, contrasting with the Pallatanga Fault system that does offset Quaternary formations [Baize *et al.*, 2014].

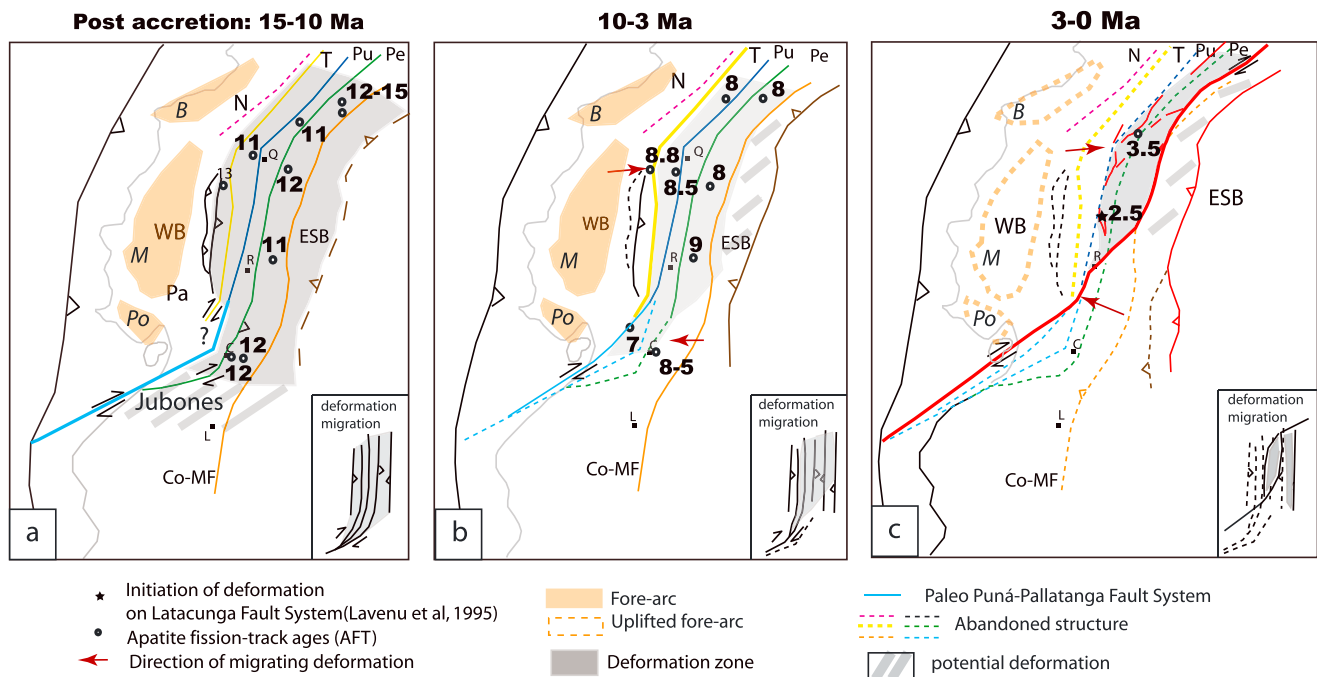


**Figure 4.** Compiled thermochronological data (<15 Ma) superimposed on suture and fault map, illustrating the overall evolution of exhumation as described in the literature. Apatite fission-track ages are from Steinmann et al. [1999], Spikings et al. [2000], Spikings et al. [2001], Winkler et al. [2005], and Spikings et al. [2010] The inset cartoon illustrates the large-scale evolution and eastward migration of the deformation through times. Fore-arc basin localization after Deniaud [1999]. Progreso Basin: Po; Manabí Basin: M; Borbón Basin: B; Naranjal Fault: N; Western Andean Belt: WB; Pujilí Melange; Peltetec fault: Pe; Naranjal fault: N; Toachi shear zone: T; Cities: Quito: Q; Riobamba: R; Cuenca: C; Guayaquil: G, Latacunga: L; Jubones: Ju; Cosanga and Mendez faults: Co-MF.

not affect recent volcanic rocks of Chimborazo volcano farther to the north (Figure 3). During the Miocene, fore-arc marine basins developed in the present-day coastal region (Progreso, Manabí, and Borbón basins) [Benítez, 1995; Deniaud et al., 1999; Witt et al., 2006]. The corresponding marine sediments were uplifted during the Pliocene, and the fore-arc basins were finally filled up with continental deposits during the Pleistocene. During the Mio-Pliocene, the Gulf of Guayaquil basin opened as a consequence of the NAS escape to the north and was characterized by moderate subsidence and sedimentation rates [Benítez, 1995; Deniaud et al., 1999]. However, for the Pleistocene, the Guayaquil submarine basins exhibit up to 4 km of sediment that accumulated during the past 1 Ma. They are testimony of an increase of subsidence and a high deposition rate varying between 700 m/Ma and 8600 m/Ma. [Deniaud et al., 1999]. The offshore Pliocene series shows no significant variations in thickness throughout the Gulf of Guayaquil area, suggesting that no significant vertical tectonic deformation occurred between 5.2 and 1.8–1.6 Ma [Benítez, 1995; Witt et al., 2006].

Thermochronological studies reveal variable exhumation rates for each Andean domain and several distinct cooling events since the Cretaceous [Spikings et al., 2001, 2010]. These exhumation phases were coeval with transpressive deformations recorded on the continent and are recorded between 75 and 30 Ma, and most importantly for our study during the last 15–10 Ma [Spikings et al., 2005]. Although spatially variable, even in a single region, the general exhumation pattern for the last 15 Ma is presented in Figure 4 [Steinmann et al., 1999; Spikings et al., 2000, 2001, 2010; Winkler et al., 2005]. Distinct periods of cooling during the late Miocene-Recent in the northern Eastern Cordillera and the Western Cordillera temporally correlate with giant alluvial fan sedimentation along the edges of the Andean massif, west or east in the Amazon foreland basin, attesting that cooling was a result of surface uplift and erosion. However, rock uplift was a result of continental deformation, although not necessarily controlled by terrain bounding faults or sutures [Spikings et al., 2001, 2010]. Since the middle to late Miocene (15 to 10 Ma), most of the domain comprising the present-day Western Cordillera, Cordillera Real, and Interandean Valley has been exhumed from southern Ecuador to Colombia (Figures 1 and 4) [Steinmann et al., 1999; Spikings et al., 2000, 2001; Spikings and Crowhurst, 2004]. Miocene and younger exhumation of both the Western Cordillera and the Cordillera Real has been constrained by Apatite Fission Track (AFT) analysis (Figure 4) and tectonic studies (Figure 3). For example, highly deformed

**Table 1.** Crustal Earthquakes, Historical, and Instrumental Associated With Important Damages<sup>a</sup>

Code Figure 5	Y/M/D	Event Name	Magnitude	Code Figure 5	Y/M/D	Event Name	Magnitude
1	1587/08/31	Guayllabamba	6.4 $M_I$	12	1955/7/20	Atahualpa	6.1 $M_I$
2	1698/6/20	Ambato	7.3 $M_I$	13	1960/7/30	Pasa	5.7 $M_I$
3	1797/2/4	Riobamba	7.6 $M_I$	14	1962/11/16	Cusubamba	5.9 $M_I$
4	1868/8/16	Ibarra	7.3 $M_I$	15	1976/10/6	Pastocalle	5.7 $M_b$
5	1868/8/15	El Angel	6.6 $M_I$	16	1987/3/6	Salado-Reventador	7.1 $M_w$
6	1911/9/23	Cajabamba	6.2 $M_I$	17	1990/8/11	Pomasqui	5.3 $M_w$
7	1914/5/31	Antisana	6.4 $M_I$	18	1996/3/28	Pujilí	5.9 $M_w$
8	1929/7/25	Murco	5.9 $M_I$	19	1834/1/20	Sibundoy <sup>b</sup>	7.7 $M_s$
9	1938/8/10	Sangolqui	5.8 $M_I$	20	1923/12/14	Cumbal <sup>b</sup>	7.0 $M_s$
10	1944/9/15	Toacazo	5.7 $M_I$	21	1947/7/14	Guaitara <sup>b</sup>	7.0 $M_s$
11	1949/8/5	Pelileo	6.8 $M_s$				

<sup>a</sup> $M_I \sim M_w$  magnitude after Beauval *et al.* [2010].  $M_s$  surface wave magnitude,  $M_w$  seismic moment magnitude,  $M_b$  body-waves magnitude.

<sup>b</sup>Southern Colombia crustal historical earthquakes, data after Calvache [2007] and Espinosa [2010].

rocks from the Toachi shear zone (Western Cordillera) were rapidly cooled and exhumed at 5 Ma, and Jurassic basement rocks located close to the Chingual Fault in northernmost Ecuador cooled rapidly since 6 to 4 Ma [Spikings *et al.*, 2000, 2005] (Table 1).

Between 9 Ma and 5 Ma, the eastward migration of the uplifted and deformed areas was coeval with the initiation of the deformation of the Subandean zone (Figure 4). AFT ages from the igneous basement rocks from the Subandean Zone suggest that they were rapidly cooled during the late Miocene [Ruiz, 2002; Spikings *et al.*, 2010]. The entire extent of the Western Cordillera located west of the Pujilí Suture exhumed rapidly at 15 Ma (Figure 4). Apatite (UeTh)/He data reveal rapid cooling and exhumation (from 2.3 km to the present surface) [Spikings and Crowhurst, 2004] in the northern part of the Eastern Cordillera, commencing around 5 to 3 Ma, although this has not been detected south of  $51^{\circ}30'$ . In parallel, the eastern Western Cordillera also started exhuming in the late Miocene. This spatial variation in exhumation is attributed to dextral transcurrent reactivation of the favorably oriented and mechanically weak sutures, leading to exhumation in the Western Cordillera. This micro-block played the role of an indenting buttressing block, and Spikings *et al.* [2010] attribute the driving force to pulses of compressive stress during the collision of the Carnegie Ridge with the upper plate, starting at 15 Ma.

### 1.3. Neotectonic Homogeneous Map and New Data: Major Fault Systems Description

Here we compile individual and local tectonic studies from the literature and present them on a new comprehensive map based on an analysis of tectonic geomorphology (Figure 5). The faulting patterns observed across Ecuador appear to preserve different stages in the development of these oblique-slip fault systems, and thus, it is important to describe their evolution through time. On this new tectonic map of Ecuador, we present here the complete data set of active faults in Ecuador (Figure 5, neotec-opendata.com). It is compiled from our analysis of a range of Quaternary markers: alluvial terraces, scarps, moraines, and volcanic formations, as well as detailed local field surveys and paleoseismic trenches [Ego, 1995; Lavenu *et al.*, 1995; Audin *et al.*, 2003; Equez *et al.*, 2003; Tibaldi *et al.*, 2007; PMA, 2009; Baize *et al.*, 2014; Alvarado *et al.*, 2014]. Figure 5a displays major active fault systems on the shaded topographic map of Ecuador (SRTM 90 m). In the following, we summarize the different major active systems from north to south, together with their main characteristics in terms of kinematics.

#### 1.3.1. The Chingual Fault System

In northern Ecuador, the Chingual fault runs along the Eastern Cordillera northeastward [Tibaldi and Ferrari, 1992; Ego *et al.*, 1996] and connects to the La Sofia and Río Cofanes faults. Morphological and geodetic evidence of transpression combined with  $^{14}\text{C}$  radiometric dating provide reliable slip rate measurements for the Quaternary time period [Ego, 1995]. Slip rates along the Chingual system range from 7 to 10 mm/yr [Ego, 1995; Tibaldi *et al.*, 2007]. Using the Euler pole from Nocquet *et al.* [2014] (longitude  $-83.40^{\circ}\text{E}$ , latitude  $15.21^{\circ}\text{N}$ , angular velocity  $0.287^{\circ}/\text{Ma}$ ), the motion predicted for the NAS with respect to Stable South America suggests movement of 8.5 mm/yr in a  $\text{N}65^{\circ}\text{E}$  direction (at longitude  $76.79^{\circ}\text{W}$ , latitude  $1.24^{\circ}\text{N}$ ) and is in agreement with the Quaternary slip rates. This rate of movement indicates that the Chingual fault is the major fault accommodating the motion of the NAS, the contribution of all other faults being negligible

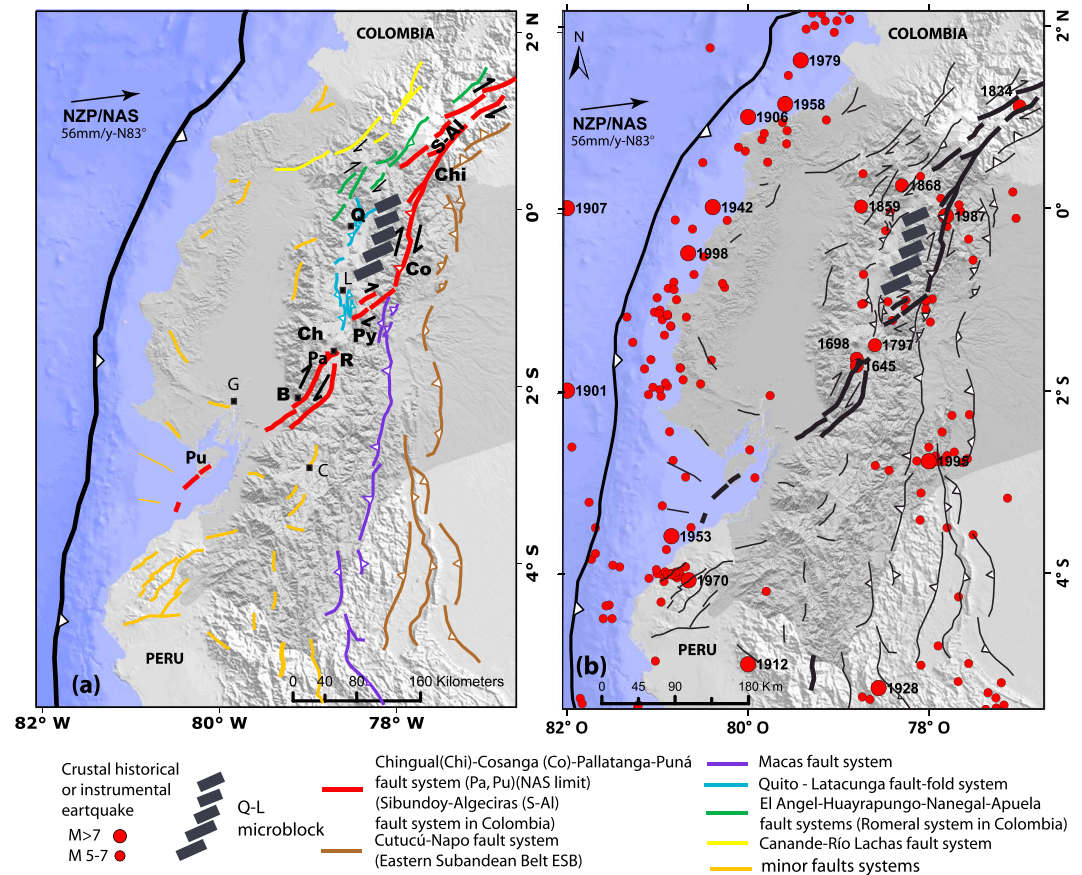


**Figure 5.** (a) Active fault map of Ecuador: Major active fault systems and their Quaternary kinematics. (b) Instrumental and historical crustal seismicity in Ecuador (>40 km deep, and magnitude > 5). Active fault segments [Alvarado, 2012] are reported on 30 m digital elevation model (DEM) developed by Souris [2003]. Historical data compiled after Beauval et al. [2010] for Ecuador and after Calvache [2007] and Espinosa [2010] for Colombia (see Table 1). Riobamba; R; Quito; Q; Bucay; B; Chimborazo volcano; Ch; Pisayambo Faults; Py; Pallatanga; Pa; Puna; Pu.

in terms of kinematics. The Chingual fault system extends to Colombia through the Afiladores-Sibundoy-Algeciras Fault System [Paris et al., 2000; Velandia et al., 2005] (Figures 1 and 5a).

### 1.3.2. The Cosanga-Salado Fault System

The Cosanga segment (Figures 1 and 5a) follows the entrenched valley of the Río Cosanga and trends N-S, showing compressive components of movement during the Quaternary period. The successive active fault segments can be followed northward in the Río Quijos valley. The Cosanga segment shows a mainly reverse offset with a dextral secondary component and connects northward to the Salado fault segments. The Salado reverse fault is associated to crustal earthquakes and among them the  $M_w$  7.0 event in 1987 [Gajardo et al., 2001; Kawakatsu and Proaño, 1991]. The active Cosanga segment is located close to the ancient Cretaceous-age Cosanga fault, defined by Aspden and Litherland [1992], and considered to represent the western limit of the cratonic front, probably active during the Middle to Late Jurassic. Pratt et al. [2005] suggest that this fault had a reverse dip-slip movement, during the Tertiary (Miocene-Pliocene?).

### 1.3.3. The Pallatanga Fault System

The Pallatanga segment (Figures 1 and 5a) is the southern extension of the Pujilí Fault [Hughes and Pilatasig, 2002]. It crosscuts the Western Cordillera, and several sutures are shown in Figure 3. This fault system extends east of the Gulf of Guayaquil [Winter et al., 1993] and about 200 km to the NE across the Interandean Valley, up to the foot of Chimborazo volcano, following the entrenched valley of the Río Pangor. Holocene slip rates have been proposed to be 2.5–4.6 mm/yr [Winter et al., 1993; Baize et al., 2014]. This value is 30% of the prediction (7.1 mm/yr, N47E) derived from GPS for the relative motion of the NAS with respect to the Inca Sliver, using the Euler poles from Nocquet et al. [2014]. To the Southwest, the Pallatanga fault system can be traced

down toward the coastal plain. It forms at least two restraining bends and then connects to the Puná active fault segments on the Puná Island [Dumont *et al.*, 2005].

#### 1.3.4. The Puná Fault System

The Puná fault system (which can be traced to the Miocene [Dumont *et al.*, 2005]) represents a segment of the southern boundary of the NAS. This system includes several active segments: the Zambapala flower structure [Lions, 1995] and the Santa Clara fault [Dumont *et al.*, 2005]. Farther to the south, the Amistad flower structure in the Gulf of Guayaquil [Benítez, 1995; Deniaud, 1999] is considered to represent the offshore continuation of the main Pallatanga-Puná fault system (Figure 5a). The Gulf of Guayaquil itself is a complex pull-apart structure, bordered by secondary NW-SE normal faults and a very thick sedimentary package of Pleistocene age. Witt and Bourgois [2010] suggest that the opening of the Gulf of Guayaquil marks the onset of a northward drift of the NAS, in agreement with the development of local extensional tectonics bounding this basin. Dumont *et al.* [2005] proposed a Holocene minimal mean slip rate of 5.8–8 mm/yr for the Zambapala segment (at longitude 80.23°W, latitude 3°S), in agreement with the prediction of 7.1 mm/yr in a N52°E direction, derived from our GPS data.

#### 1.3.5. Macas Fault System

In Southeastern Ecuador, the Macas fault system bounds the Cordillera Real on its western flank. Its northern prolongation was probably part of the Méndez fault (Figures 1 and 5a) [Aspden and Litherland, 1992]. Morphological evidence suggests a compressional deformation toward the Subandean domain to the east [Bès de Berc *et al.*, 2005], although no significant instrumental or historical crustal seismicity ( $M > 4$ ) appears to be related to this structure (Figure 5b).

#### 1.3.6. Napo-Cutucú Fault System (Eastern Subandean Belt)

Mesozoic to Cenozoic strata are involved in the fold-and-thrust belt of the Subandean region (Figures 1 and 5a). The Cutucú-Napo Fault System represents the easternmost belt of deformation in Ecuador. Mostly involving thin-skinned tectonics, the Cutucú-Napo Fault System is active from its northern part in the Napo region to the Puyo and Pastaza regions, affecting the Quaternary drainage network [Bès de Berc, 2003]. The Subandean region deformation is likely related to the presence of a local-scale thrust ramp underlying the Subandean Zone and emerging locally in front of the Cutucú-Napo Fault System [Bès de Berc, 2003; Legrand *et al.*, 2005]. The easternmost thrusts characterize here the eastward propagation of a continental accretionary wedge as observed to the South in the Peruvian Andes [Gil *et al.*, 2001]. This structure is associated with the Macas  $M_w$  7.1 reverse crustal earthquake in 1995 [Legrand *et al.*, 2005].

#### 1.3.7. Quito-Latacunga Fault System QL

This fault system combines the Quito Fault System (QFS, Figures 1 and 5a) and the Latacunga Fault System defined after Lavenu *et al.* [1995], Ego [1995], and Fiorini and Tibaldi [2011]. These fault segments affect the whole pile of Quaternary to Holocene layers that fill the Interandean Valley, attesting to the ongoing blind thrusting in this region. The QFS exhibits evidence for a slip rate of 4–5 mm/yr shortening estimated from GPS, whereas the Latacunga fault system shows a slower rate of  $\approx 1$  mm/yr [Alvarado *et al.*, 2014] (Figure 7). The QFS is expressed by parallel strands of folds located above major west dipping, blind, en echelon thrust faults. To the South, the Latacunga fault system eventually terminates along the Pallatanga Fault [Baize *et al.*, 2014]. To the west, the mean N-S strike of the Quito and Latacunga faults rotates to a more NNE-SSW azimuth, and the faults are apparently rooted in the deeper Pujilí Suture zone.

### 1.4. Neotectonic Summary

Assessment of the geometry and location of active structures in the region has proven challenging to date in Ecuador, primarily because of the dense vegetal cover and the low crustal instrumental seismicity registered since 1960 [Beauval *et al.*, 2010]. However, systematic analysis of fault size, geometry, and geomorphic displacement reveals a hierarchy of tectonic features (PMA, neotec-opendata.com). The Chingual-Cosanga-Pallatanga-Puná fault system (CCPP) represents the best developed fault system in Ecuador (Figure 5a). It constitutes the eastern tectonic boundary of the North Andean Sliver and connects three different transpressive and reverse subsystems. It was first suggested by Ego *et al.* [1996] to be associated with a major restraining bend in Ecuador or to secondary active faults, lying east of a main transfer zone described by Winkler *et al.* [2005]. The CCPP is about 800 km long, from the Gulf of Guayaquil in southwestern Ecuador to the eastern side of Cordillera Real at the Ecuador-Colombia border (Figure 1). Its geomorphology is expressed by one or more parallel fault segments striking N-S to NE-SW. The North-South trending segments localize the hypocenters of several major historical earthquakes as well as instrumental seismicity as described below. However, the active tectonic synthesis presented above suggests the existence of an additional microblock:

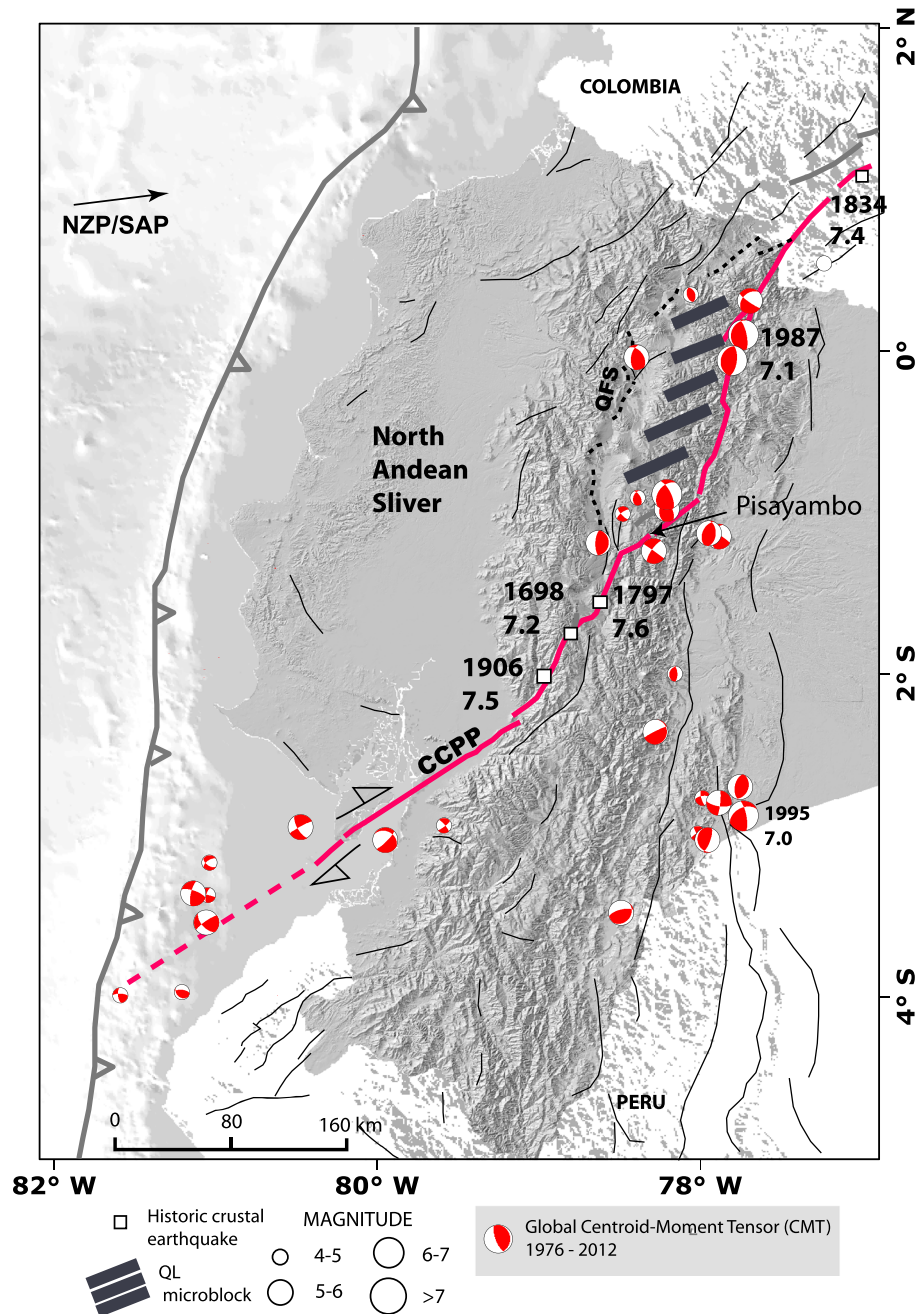


**Figure 6.** Earthquake focal mechanisms in Ecuador (magnitude > 4 and depth < 40 km), reported on the active fault map (this study) of Ecuador. Time period: 1976–2012 for instrumental CMTs and *Beauval et al.* [2010] for historic data sets; data sources: global centroid moment tensor (CMT) [*Suarez et al.*, 1983; *Mendoza and Dewey*, 1984; *Segovia and Alvarado*, 2009; *Alvarez*, 2003; *Manchuel et al.*, 2011; *Instituto Geofísico-EPN Database*, 2012]. First stress tensor, for crustal earthquakes after *Segovia and Alvarado* [2009]. Chingual-Cosanga-Pallatanga-Puná fault system (CCPP).

the Quito-Latacunga Microblock (Figure 5a), which extends from east to west between the Cosanga and Quito-Latacunga fault systems. The Quito-Latacunga Microblock southern limit coincides with the Pisayambo fault zone (Figure 5a) and its northern limit with the SW tips of the Chingual fault. Indeed, several branches of the Algeciras-Sibundoy-Chingual Fault system display evidences of a southwestward continuation into the Interandean Valley, with NNE-SSW trending individual faults, such as the Santa Barbara and San Gabriel segments. We discuss the potential existence of this microblock using seismicity and GPS data and its role in terms of the evolution of the upper plate deformation through time.

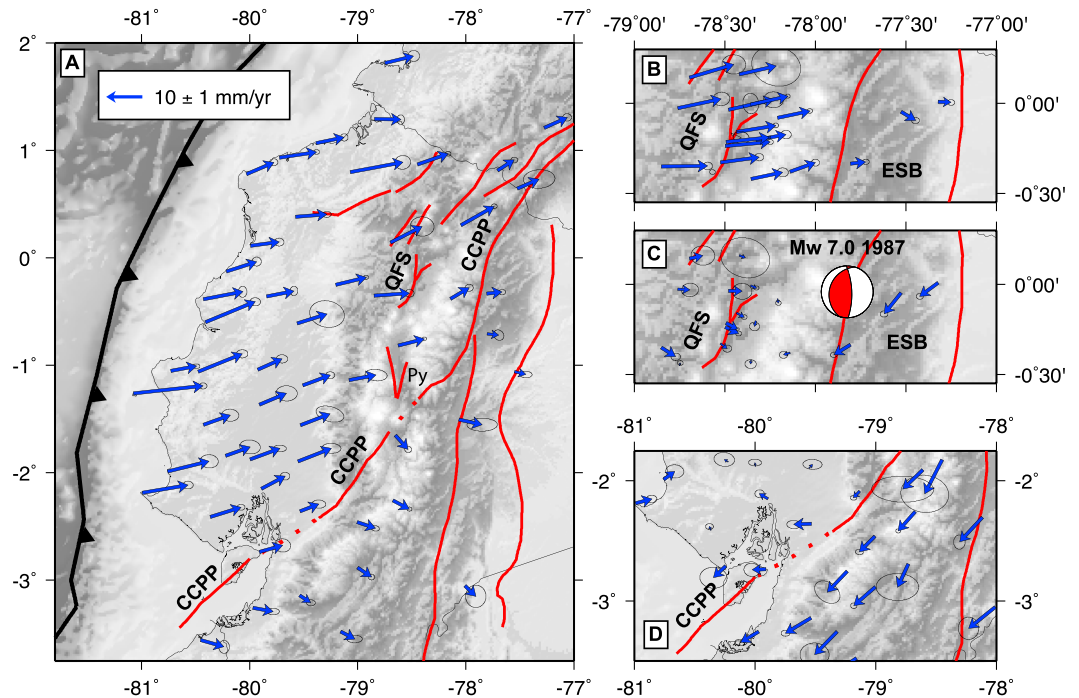


**Figure 7.** (a) GPS horizontal velocity field with respect to Stable South America [Nocquet *et al.*, 2014]. (b) GPS horizontal velocity field with respect to the Interandean Valley (see text for details), together with the focal mechanism derived by Kawakatsu and Proaño [1991] for the 1987 ( $M_w$  7.0) earthquake. (c) GPS horizontal velocity field with respect to the NAS. Chingual-Cosanga-Pallatanga-Puná Fault System: CCPP; Quito Fault System: QFS; Py: Pisayambo zone; Eastern Subandean Belt: ESB.

### 1.5. Seismotectonics and Focal Mechanisms

Ecuador has experienced numerous earthquakes in the historical and instrumental periods [Beauval *et al.*, 2013] (Figure 5b). Many of the faults documented in this paper constitute hazards for local populations, including the cities of Quito and Guayaquil (Figures 5a and 5b). In Ecuador, local seismic station coverage is dense enough to allow for determination of hypocentral depths (Figure 5b, e.g., RENSIG [Segovia and Alvarado, 2009; Beauval *et al.*, 2010]). The RENSIG provides instrumental locations, magnitudes, and focal mechanisms (Instituto Geofísico, Escuela Politécnica Nacional, EPN). We compiled and revised published fault plane solutions [Calahorrano, 2001; Alvarez, 2003; Troncoso, 2009; Segovia and Alvarado, 2009; Manchuel *et al.*, 2011; Instituto Geofísico-EPN, 2012] centroid moment tensor (CMT) (Figure 6).

Since 1988, the local seismic network (RENSIG) has detected more than 44,000 tectonic events, 14% of them with magnitudes  $\geq 4$ , with about 300 focal mechanisms (Figure 5b). Focal mechanisms of shallow crustal earthquakes ( $M > 4$  and less than 40 km deep, depth error  $\pm 10$  km), which occurred in Ecuador in the last 25 years, define distinct zones of seismic activity and stress regime (Figure 6). Strike-slip faulting dominates within and near the Gulf of Guayaquil in agreement with the right-lateral motion of the Puná segment of the CCPP. Predominant reverse faulting occurs along the Cosanga-Chingual segment, in agreement with the fault style observed in this area and the large-scale kinematics derived from GPS. Finally, a few significant earthquakes have occurred in the Interandean Valley, including the recent 12 August 2014,  $M_w$  5.1 Quito earthquake.

The location of the focal mechanisms and large historical earthquakes enlightens the CCPP as a major boundary. The change in earthquake focal mechanisms is coherent with the relative motion of the NAS with respect to its surrounding domains: pure right-lateral strike-slip motion occurs between the NAS and the Inca sliver from the Gulf of Guayaquil to the eastern Cordillera, and a mainly transpressive motion occurs between the NAS and the Subandean domain. As secondary features, active faults and their focal mechanisms are found west and south of the Interandean Valley, along the Quito-Latacunga fault system. There, Quaternary and ongoing movements are mainly compressive with a right-lateral component compatible with longer-term data documented through previous geomorphic analysis [Lavenu *et al.*, 1995; Fiorini and Tibaldi, 2011]. The Pisayambo area marks the tectonic transition zone between the NS Cosanga and NE-SW Pallatanga segments and the southern tip of

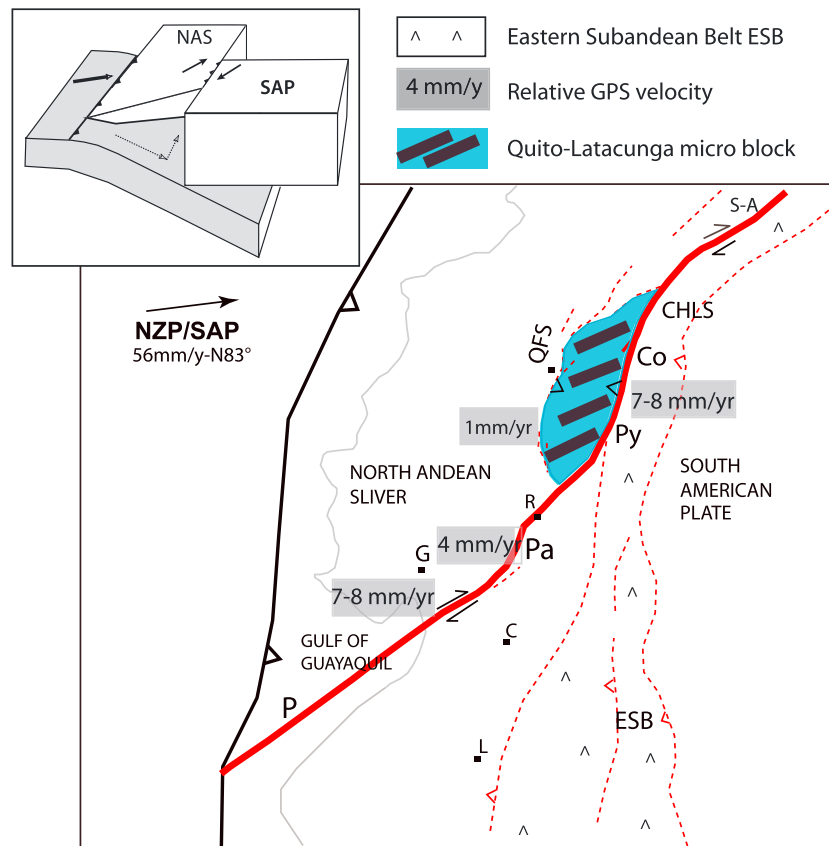


**Figure 8.** Final model proposed in this study, showing the present-day eastern limit of the North Andean Sliver. In light blue the Quito Latacunga microblock. New model for the extrusion of the NAS. The velocities correspond to GPS measurements. Puná: P; Pallatanga: Pa; Chingual-La Sofía: CHL; Sibundoy-Algeciras: S-A; Eastern Subandean Belt: ESB; Guayaquil: G; Loja: L; Convergence Nazca-South American Plates: NZP/SAP.

the Latacunga fault system. The Pisayambo area is characterized by a high level of background seismicity, and swarms of distributed crustal microseismicity, account for 2–5% of the number of >4 magnitude earthquakes registered in Ecuador [Troncoso, 2009; Guillier *et al.*, 2001]. However, geomorphic analysis based on DEM or precise aerial images does not show major outcropping tectonic structures but rather show several diffuse active second-order fault segments [Alvarado, 2012; Audin, 2013; neotec-opendata.com], associated with the activity of a NE-SW strike-slip fault system involving numerous kilometer-scale fault segments. Finally, the level of significant earthquake is mild in the Subandean domain, a feature that contrasts with results observed in other parts of the Andes. We suggest that (1) the significant seismicity is clearly associated with faults having clear geomorphological expressions, aside from the Pisayambo area; (2) focal mechanism support the hypothesis of an additional secondary Quito-Latacunga microblock; and (3) the Interandean Valley fault system, the strike-slip Pallatanga fault segment, and Cosanga reverse fault meet in the Pisayambo area, showing a high level of microseismicity, probably associated with a diffuse deformation mode.

### 1.6. GPS Results

Nocquet *et al.* [2014] show that at the regional scale, the present-day kinematics of the Andes and its western margin is dominated by the diverging motion of the NAS and the Inca Sliver, the latter encompassing southern Ecuadorian and Peruvian Andes and their margin. Here we present new GPS data along the Cosanga segment (Figure 7) and the Pallatanga-Puná segment (Figure 8), together with data used in Alvarado *et al.* [2014]. The results are based on campaigns data, first measured in the 1990s by the Instituto Geográfico Militar, which we remeasured in 2009 and 2011. All campaign sites have a minimum observation period of 10 years, leading to velocity determined at the 1 mm/yr level, or less. The full description of the GPS processing is provided in Nocquet *et al.* [2014] (supporting information). With respect to a Stable South America Reference Frame

(Figure 7a), a clear gradient is seen in the eastern component of the velocity field from  $\sim 12.5$  mm/yr in the western Cordillera, 8 mm/yr in the Interandean Valley east of Quito, and finally 3–4 mm/yr for sites located on the Subandean fold-and-thrust belt. Furthermore, the overall shortening is accommodated over short distances that correlate spatially with the active faults. About 4–5 mm/yr are accommodated across the Quito Fault System (QFS, Figure 7b) [Alvarado *et al.*, 2014], and a large gradient occurs between sites PAPA (7.5 mm/yr) located in the eastern Cordillera and ELCH (4.2 mm/yr) located just east of the Cosanga fault trace. In order to better visualize the motion accommodated by the Cosanga fault, we show in Figure 7c the same velocity field now expressed with respect to the Interandean Valley, as defined using the PAM1, PAPA, PINT, REDO, SALV, and SBAR stations, which shows little internal deformation (weighted root-mean-square (wrms) = 0.6 mm/yr). In that reference frame, clear relative motion is seen between the Subandean Fold Belt and the Interandean Valley. About 7 mm/yr of SW-ward, right-lateral transpressive motion is clearly seen. The lower velocities found for site ELCH probably reflects interseismic strain accumulation close to the fault. Therefore, relative motion between the East Subandean Belt and the Interandean Valley appears to be highly localized. This relative motion derived from GPS is further consistent with the focal mechanism derived for the 1987  $M_w = 7.0$  earthquake, the largest event that occurred during the instrumental period in Ecuador [Kawakatsu and Proaño, 1991].

Figure 7d shows the velocity field for the area located east of the Gulf of Guayaquil, expressed in the NAS reference frame as defined in Nocquet *et al.* [2014]. The area encompasses the Puná and Pallatanga segments of the CCPP. The velocity field shows a clear pure right-lateral strike-slip motion of the Inca sliver with respect to the NAS. Although there is no clear geomorphologic trace of the fault between the Pallatanga and the Puná segments, GPS predicts that  $\sim 8$  mm/yr of relative motion over a distance less than 50 km is accommodated there, providing evidence that the CCPP is the major tectonic structure delimiting the southern limit of the NAS.

## 2. Discussion

### 2.1. Sutures Not Systematically Reactivated as Continental Slivers Boundaries

Early studies of the northern Andes and the southern Caribbean proposed the Dolores-Guayaquil Megashear as a major boundary decoupling crystalline rocks from accreted oceanic crust [Campbell, 1968; Case *et al.*, 1968; Case *et al.*, 1971]. In Ecuador, the major limit was first proposed to follow the foothill of the western Cordillera [Campbell, 1968]. Further detailed studies showed that the main suture zone was actually following the eastern side of the western Cordillera [Kerr *et al.*, 2002] and that the correct definition of this suture corresponds to Pujilí Melange [Hughes and Pilatasig, 2002]. Audemard and Audemard [2002] suggested that this limit merges with the Romeral in Colombia and Bocono faults in Venezuela, further attested by Molnar and Dayem [2010]. This limit is still widely used, and for instance, the Dolores-Guayaquil Megashear zone following the western Cordillera is the limit included in the global compilation of tectonic plates and microplates from Bird [2003]. While the segment from the Gulf of Guayaquil to the Cordillera remains correct, our study clearly demonstrates that the currently active major boundary should be  $\sim 80$  km east of the former accepted limit for central-northern Ecuador and southern Colombia. The location of the present-day boundary of the NAS demonstrates that sutures are not always reactivated and that other factors control the localization of deformation.

### 2.2. The Influence of the Volcanic Arc on Localizing the Oblique Deformation

An alternative explanation for the current location of deformation is the thermal softening of the underlying crust associated with Quaternary volcanism. This process has been invoked, for instance, in Chile for the Chiloe fore-arc sliver [Wang *et al.*, 2007] or Central America [La Femina *et al.*, 2009] where the major fault system accommodating the oblique convergence runs along the volcanic arc. Unlike other subduction volcanic settings, Ecuador has a volcanic arc width that exceeds 90 km from the western Cordillera to the Subandean domain. Most of the active volcanic arc in Ecuador lies west of the narrow CCPP tectonic limit. The two closest volcanic centers are a recently discovered cluster of small Quaternary volcanoes closed to the Cosanga segment [Mothes *et al.*, 2013] and the active Reventador and Sumaco volcanoes that lies immediately north and east of Cosanga, respectively. Although there might be some control of the location of the major fault system, the volcanic activity is not as localized as in others Andean sectors [e.g., Melnick *et al.*, 2009].

### 2.3. Update of the Tectonic and Geodynamic Models for Ecuador

During the last two decades, several models have been proposed to explain the tectonic activity observed in Ecuador [e.g., Tibaldi and Ferrari, 1992; Lavenu *et al.*, 1995; Ego *et al.*, 1996; White *et al.*, 2003; Dumont *et al.*,

2005; Winkler *et al.*, 2005; Witt and Bourgois, 2010]. Previously proposed models fall into two conceptual classes. According to the first category of models, the tectonic activity is distributed along four major fault types: reverse, parallel, N-S-trending fault systems, active in the higher Andes between the western Cordillera and the Subandean region, which accommodate diffuse deformation in the Northern Andean Sliver during its northward “escape” [e.g., White *et al.*, 2003]. A second category of models considers a single restraining belt model proposed by Ego *et al.* [1996], with the present-day active restraining belt cutting through the Interandean Depression, next to Quito. Strike-slip faults are a frequent component of active tectonic regions undergoing continental shortening [e.g., Tapponnier and Molnar, 1979; Jackson and McKenzie, 1984]. They accommodate shortening by translation of continental slivers, by partitioning of dip-slip and strike-slip components, or through a combination of strike-slip faulting and rotations of microblocks around vertical axis [e.g., Cunningham and Mann, 2007]. Consequently, restraining bends occur where a localized component of shortening is introduced due to changes in fault strike. The faulting within these restraining bends is often diffuse and may evolve rapidly [e.g., Cunningham and Mann, 2007]. At both crustal and regional scales, previously published models rely on partial geological and/or geophysical data, thus having only local or short-term temporal significance, if considered independently. The model proposed by Ego *et al.* [1996] would imply NNE-SSW extension in the Interandean Depression north of Quito. This extension is neither observed in the morphology, the focal mechanisms, nor seen in the GPS data (Figures 2 and 7a). Similarly, the horse-tail termination model of Soulas *et al.* [1991] would imply N-S extension on faults, which, however, do not show any geomorphic signature or Quaternary tectonic activity. Besides, both categories of models failed to predict the high and localized motion that we observe along the CCP, which defines the present-day major boundary of the NAS. Our new kinematic model (Figure 8) is based on multidisciplinary observations of geologic, geomorphic, seismic, and geodetic data that provide a new coherent and integrated interpretation at imbricated spatial and time scales. It is compatible with the idea of a restraining bend whose eastern boundary would accommodate 80–90% of the relative motion.

#### 2.4. Narrowing Restraining Bend, Localized Tectonics, and Surface Uplift Timing

The cordilleran exhumation as well as the observed horizontal deformation in Ecuador appears also to be intimately linked with the development of evolving tectonic configurations through time. We propose here a coherent interpretation, which involves successively narrowing restraining bends rather than a single one. Also, the principal tectonic shortening or transpression between the former trench location and the stable craton appears to have migrated eastward from the Western Cordillera to the Cordillera Real since 15 Ma. Hence, the transpressional style described for most of the CCP should represent the dominant deformation style for the Quaternary. Our model does not fit with the previous hypothesis of a Pliocene restraining belt [Ego *et al.*, 1996] nor with a compressive graben [Lavenue *et al.*, 1992; Winkler *et al.*, 2005] but rather with a major unique fault system, bounding rigid blocks, and localizing most of the deformation. Within this interpretation, the existence of the Quito-Latacunga block would correspond to a residual of the previous stages of the evolution, with the deformation now being transferred along its eastern boundary.

We postulate that dextral transpressional deformation is the dominant process in the structural development and uplift of the Northern Andes in Ecuador for more than 15 Ma, as opposed to the mainly compressive deformation style recorded in Northern Peru [Naeser *et al.*, 1991]. Modeling the structure of the northern Andes as a dextral transpressional margin requires a temporal evolution of the NASA's southeastern boundary, and associated restraining bends, into a more mature fault system, which suggests the establishment of a localized continental plate boundary. This plate boundary developed and localized since the Quaternary [Benitez, 1995]. The opening of the Gulf of Guayaquil attests for its activity during the past 1.8–1.6 Ma [Deniaud *et al.*, 1999].

Seismicity distribution at depth indicates that the allochthonous terrains are dipping eastward, constituting a crustal accretionary prism, which indeed forms the crustal root of the Western Ecuadorian Andes [Guillier *et al.*, 2001; Jaillard *et al.*, 2002]. Following the accretions, the last tectonic episodes of activity are associated with the rapid uplift of the Cordilleras (15–0 Ma) and correspond to the initiation of continental deformation. As ongoing subduction yielded compression to the upper plate, the overthickened prism becomes rigid and is no longer able to accommodate additional compression as proposed by Bonnardot [2003]. As a consequence, at 3–0 Ma, most of the strain is transferred eastward to the Cordillera Real's inherited fault zones. Previously, from 40 to 15 Ma, deformation was concentrated along sutures and faults [Jaillard *et al.*, 2009; Spikings *et al.*, 2010]. However, as structures were reorganized with the migration of the deformation,

compression involving the Interandean Valley resulted in its rapid uplift of the Interandean Valley and that of the Cordilleras as observed between 15 and 0 Ma (see Figure 3). This rapid exhumation concluded with the coastal plain and the marine basins uplift during the Quaternary. Later on, active structures began to develop across and within the Interandean Valley, as exemplified by the activation of the Puná-Pallatanga Fault System. This NE-SW fault system cojoined also activity of the Afiladores-Sibundoy-Algeciras Fault System and began to act together with the CCPP, resulting in the progressive vanishing of the wider restraining bend. The initial restraining belt finally tended to vanish and narrow while maturing, in order to form a unique fault system as demonstrated by seismic and geodetic data. Indeed, without complete GPS and seismic data sets covering the whole length of the CCPP Fault system, the remaining active segments and the Quito-Latacunga microblock would suggest the distribution of continental deformation in and east of the Interandean Valley, as proposed by White *et al.* [2003]. These findings do not exclude the possibility that other active faults exist away from the main fault zone but suggest that their contribution to the general tectonics of Ecuador must be relatively minor. Finally, most of the continental shortening and strike-slip deformation is now demonstrated to be well localized on a single, newly defined large-scale fault system: the Chingual-Cosanga-Pallatanga-Puná Fault System.

### 3. Conclusion

We propose a new interpretation of the tectonic evolution of the northern Andes in Ecuador in the light of an extensive data set. We could constrain the present-day kinematics and discuss only the inherited geological imprint. In contrast to former studies, our compiled and new data set demonstrates the existence of a very localized, rather than distributed, intraplate continental boundary showing slip rates of  $\sim 8$  to 10 mm/yr and defined as the Chingual-Cosanga-Pallatanga-Puná fault system (CCPP). The following key results arise from this study: most active faults do not coincide with preexisting suture zones. More generally, sutures are not reactivated during the recent evolution of the deformation system. As a consequence, the accretion process does not have a strong imprint on the current deformation.

1. NAS extrusion occurs rapidly as the Nazca plate moves eastward relative to the Brazilian Shield at  $\sim 56$  mm/yr. GPS results indicate 8–10 mm/yr of northeastward motion with respect to the stable South American plate and indicate a quasi-rigid continental sliver.
2. Crustal seismic activity is high in the Northern Andes, and the occurrence of large earthquakes indicates that active transpression occurs in this region, mostly along the NE-SW striking fault systems.
3. Contrasting with others segments in the Andes, the deformation in the Subandean domain is small compared to the relative motion accommodated by the CCPP.

#### Acknowledgments

This publication was made possible thanks to the Institut de Recherche pour le Développement (IRD), which provided support to UMS 2572 LMC14 (CNRS-CEA-IRD-IRSN-Min. Culture et Comm.) and to the PhD grant of the author. ADN project (ANR-07-BLAN-143) and LMI "Séismes et Volcans dans les Andes du Nord." The data for this paper are available by contacting the first author and on the following open database, website: <http://neotec-open-data.com/webgis-e/>. Constructive reviews of a previous version helped to improve the manuscript. This contribution is part of an Ecuadorian–French cooperation program between the Instituto Geofísico, Escuela Politécnica Nacional (IG-EPN), Quito, Ecuador; Institut de Recherche pour le Développement and the UMR ISTerre in France (LMI SVAN).

#### References

- Aguirre, L. (1992), Metamorphic pattern of the Cretaceous Celica formation, SW Ecuador, and its geodynamic implications, *Tectonophysics*, 205(1-3), 223–237.
- Alvarado, A. (2012), Néotectonique et cinématique de la déformation continentale en Equateur, PhD, Université de Grenoble, France, 258 p.
- Alvarado, A., et al. (2014), Active tectonics in Quito, Ecuador, assessed by geomorphological studies, GPS data, and crustal seismicity, *Tectonics*, 33, 67–83, doi:10.1002/2012TC003224.
- Alvarez, V. (2003), Etude de la sismicité d'un secteur de la marge équatorienne, à l'aide d'un réseau de stations sismologiques à terre et en mer, DEA, Université Pierre et Marie Curie Paris VI (Paris) France.
- Amortegui, A., E. Jaillard, H. Lapiere, J.-M. Martelat, D. Bosch, and F. Bussy (2011), Petrography and geochemistry of accreted oceanic fragments below the Western Cordillera of Ecuador, *Geochem. J.*, 45(1), 57–78.
- Aspden, J., and M. Litherland (1992), The geology and Mesozoic collisional history of the Cordillera Real, Ecuador, *Tectonophysics*, 205, 187–204.
- Audemard, F., and F. Audemard (2002), Structure of the Mérida Andes, Venezuela: Relations with the South America-Caribbean geodynamic interaction, *Tectonophysics*, 345, 299–327.
- Audin, L. et al. (2013), Comment to "Open-source archive of active faults for northwest South America" by Gabriel Veloza, Richard Styron, Michael Taylor, and Andres, *GSA Today*, 23(10), e24–e25, doi:10.1130/GSATG169C.1.
- Audin, L., G. Hérail, R. Riquelme, J. Darrozes, J. Martinod, and E. Font (2003), Geomorphological markers of faulting and neotectonic activity along the western Andean margin, northern Chile, *J. Quat. Sci.*, 18(8), 681–694.
- Baize, S., L. Audin, T. Winter, A. Alvarado, L. Pilatasig, M. Taipei, P. Reyes, P. Kauffmann, and H. Yepes (2014), Paleoseismology and tectonic geomorphology of the Pallatanga fault (Central Ecuador) a major structure of the South-American crust, *Geomorphology*, doi:10.1016/j.geomorph.2014.02.030.
- Bauval, C., H. Yepes, W. Bakun, J. Egred, A. Alvarado, and J. C. Singaicho (2010), Locations and magnitudes of historical earthquakes in the Sierra of Ecuador (1586–1996), *Geophys. J. Int.*, doi:10.1111/j.1365-246X.2010.04569.x.
- Bauval, C., H. Yepes, P. Palacios, M. Segovia, A. Alvarado, Y. Font, J. Aguilar, L. Troncoso, and S. Vaca (2013), An earthquake catalog for seismic hazard assessment in Ecuador, *Bull. Seismol. Soc. Am.*, 103(2A), 773–786, doi:10.1785/0120120270.
- Beck, M. (1991), Coastwise transport reconsidered: Lateral displacements in oblique subduction zones, and tectonic consequences, *Phys. Earth Planet. Int.*, 68(1-2), 1–8.

- Benítez, S. (1995), Evolution géodynamique de la province côtière sud-équatorienne au Crétacé supérieur-Tertiaire, *Géologie Alpine*, Université Joseph Fourier (Grenoble) France, 71, 3–163.
- Bès de Berc, S. (2003), Tectonique de chevauchement, surrection et incision fluviale (exemple de la zone subandine équatorienne, haut bassin amazonien) PhD, Université Toulouse III, pp. 224.
- Bès de Berc, S., J. Soula, P. Baby, M. Souris, F. Christophoul, and J. Rosero (2005), Geomorphic evidence of active deformation and uplift in a modern continental wedge-top-foredeep transition: Example of the eastern Ecuadorian Andes, *Tectonophysics*, 399, 351–380.
- Bird, P. (2003), An updated digital model of plate boundaries, *Geochem. Geophys. Geosyst.*, 4(3), 1027, doi:10.1029/2001GC000252.
- Bonnardot, M.-A. (2003), Modélisation numérique des Andes d'Equateur: Des accrétiens océaniques à la déformation continentale (80–0 Ma), 35 pp., DEA, Université Savoie, France.
- Brooks, B., M. Bevis, R. Smalley, E. Kendrick, R. Manceda, E. Lauria, R. Maturana, and M. Araujo (2003), Crustal motion in the Southern Andes (26°–36°S): Do the Andes behave like a microplate?, *Geochem. Geophys. Geosyst.*, 4(10), 1085, doi:10.1029/2003GC000505.
- Calahorrano, A. (2001), Estudio del origen del enjambre sísmico de la zona norte de la ciudad de Quito, durante 1998–99, Ing. thesis, Escuela Politécnica Nacional Quito Ecuador, pp. 190.
- Calvache, M. (2007), Pasto, in *Entorno Natural de 17 Ciudades de Colombia*, edited by M. Hermelin, 344 pp., Fondo Editorial Universidad EAFIT, Medellín, Colombia.
- Campbell, C. J. (1968), The Santa Marta wrench fault of Colombia and its regional setting, 4th Caribbean Geo. Conf. Trans., Port of Spain, Trinidad y Tobago, 247–261.
- Case, J. E., I. G. Durán, A. López, and W. Moore (1968), Gravity anomalies and crustal structure, western Colombia, *Geol. Soc. Am. Spec. Pap.*, 121.
- Case, J. E., I. G. Durán, A. López, and W. Moore (1971), Tectonic investigations in Western Colombia and Eastern Panama, *Geol. Soc. Am. Bull.*, 82(10), 2685–2712.
- Costa, C., F. Audemard, L. Audin, and C. Benavente (2009), Geomorphology as a tool for analysis of seismogenic sources in Latin America and the Caribbean, in *Natural Hazards and Human-Exacerbated Disasters in Latin America*, edited by E. Latrubesse, pp. 30–46, Elsevier.
- Cunningham, W. D., and P. Mann (2007), Tectonics of strike-slip restraining and releasing bends, *Geol. Soc. London Spec. Publ.*, 290, 1–12.
- Deniaud, Y. (1999), Enregistrements sédimentaire et structural de l'évolution géodynamique des Andes Equatoriennes au cours du Néogène: Étude des bassins d'avant-arc et bilans de masse, *Géologie Alpine*, Mémoire H.S No. 32, Université Joseph Fourier Grenoble, pp. 157.
- Deniaud, Y., P. Baby, C. Basile, M. Ordoñez, G. Montenegro, and G. Mascle (1999), Ouverture et evolution tectono-sédimentaire du golfe de Guayaquil: Basin d'avant-arc néogène et quaternaire du Sud des Andes équatoriennes, *Acad. Sci. Paris*, 328, 181–187.
- Dumont, J.-F., E. Santana, W. Vilema, K. Pedoja, M. Ordoñez, M. Cruz, N. Jiménez, and I. Zambrano (2005), Morphological and microtectonic analysis of Quaternary deformation from Puná and Santa Clara Islands, Gulf of Guayaquil, Ecuador (South America), *Tectonophysics*, 399, 331–350.
- Egbue, O., and L. Kellogg (2010), Pleistocene to present North Andean 'escape', *Tectonophysics*, 489, 248–257, doi:10.1016/j.tecto.2010.04.021.
- Ego, F. (1995), Accommodation de la convergence oblique dans une chaîne de type cordillera: Les Andes de Equateur, PhD, Université de Paris-Sud (Centre d'Orsay) France.
- Ego, F., M. Sébrier, A. Lavenu, H. Yepes, and A. Eguez (1996), Quaternary state of stress in the Northern Andes and the restraining bend model for the Ecuadorian Andes, *Tectonophysics*, 259, 101–116.
- Eguez, A., A. Alvarado, H. Yepes, M. N. Machette, C. Costa, and R. L. Dart (2003), Database and map of Quaternary faults and folds in Ecuador and its offshore region, U.S. Geol. Surv. Open File Report 03-289. International Lithosphere Program's Task Group II-2 "World Map of Major Active Faults. [Available at <http://pubs.usgs.gov/of/2000/ofr-03-289/>]
- Espinosa, A. (2010), *Contribución de la Investigación a la Gestión del Riesgo en el Quindío*, *Geología-Historia de los Desastres*, Universidad del Quindío-Universidad de Ginebra (Suiza)-Academia de Ciencias, Armenia.
- Feininger, T. (1987), Allochthonous terranes in the Andes of Ecuador and northwestern Peru, *Can. J. Earth Sci.*, 24, 266–278.
- Fiorini, E., and A. Tibaldi (2011), Quaternary tectonics in the central Interandean Valley, Ecuador: Fault-propagation folds, transfer faults and the Cotopaxi Volcano, *Global Planet. Change*, 87–103.
- Fitch, T. (1972), Plate convergence, transcurrent faults and internal deformation adjacent to southeast Asia and the western Pacific, *J. Geophys. Res.*, 77, 4432–4460, doi:10.1029/JB077i023p04432.
- Gajardo, E., H. Yepes, P. Ramón, M. L. Hall, P. Mothes, and J. Aguilar (2001), Evaluación del peligro sísmico para la ruta del OCP y evaluación complementaria del peligro volcánico, Escuela Politécnica Nacional, Instituto Geofísico, Internal Report.
- Gil, W., P. Baby, and J.-F. Ballard (2001), Structure et contrôle paleogéographique de la zone subandine peruvienne, *C. R. Acad. Sci. Paris*, 333(11), 741–748.
- Gordon, R. G. (1995), Plate motions, crustal and lithospheric mobility, and paleomagnetism: Prospective viewpoint, *J. Geophys. Res.*, 100(B12), 24,367–24,392, doi:10.1029/95JB01912.
- Guillier, B., J.-L. Chatelain, E. Jaillard, H. Yepes, G. Poupinet, and J.-F. Fels (2001), Seismological evidence on the geometry of the orogenic system in central-northern Ecuador (South America), *Geophys. Res. Lett.*, 28(19), 3749–3752, doi:10.1029/2001GL013257.
- Guillot, S., and A. Replumaz (2013), Importance of continental subductions for the growth of the Tibetan Plateau, *Bull. Soc. Géol. France*, 184(3), 199–223.
- Hall, M. L., P. Samaniego, J. L. Le Pennec, and J. Johnson (2008), Late Pliocene to present volcanism in the Ecuadorian Andes, *J. Volcanol. Geotherm. Res.*, 176, 1–6.
- Hey, R. (1977), Tectonic evolution of the Cocos-Nazca spreading center, *Geol. Soc. Am. Bull.*, 88, 1404–1420.
- Hoorn, C., et al. (2010), Amazonia through time: Andean uplift, climate change, landscape evolution, and biodiversity, *Science*, 330, 927–931.
- Hughes, R., and L. Pilatasig (2002), Cretaceous and Tertiary terrane accretion in the Cordillera Occidental of the Andes of Ecuador, *Tectonophysics*, 245, 29–48.
- Instituto Geofísico-EPN (2012), Focal mechanisms data base, compiled by Segovia M., Vaca S., Alvarado A., Internal report.
- Jackson, J., and D. McKenzie (1984), Active tectonics of the Alpine-Himalayan Belt between western Turkey and Pakistan, *Geophys. J. Int.*, 77(1), 185–264, doi:10.1111/j.1365-246X.1984.tb01931.x.
- Jaillard, E., G. Hérail, T. Monfret, and G. Wörner (2002), Andean geodynamics: Main issues and contributions from the 4th ISAG, Göttingen, *Tectonophysics*, 242, 1–15.
- Jaillard, E., O. Ordoñez, J. Suárez, J. Toro, D. Iza, and W. Lugo (2004), Stratigraphy of the Late Cretaceous-Paleogene deposits of the cordillera occidental of central Ecuador: Geodynamic implications, *J. South Am. Earth Sci.*, 17, 49–58.
- Jaillard, E., P. Bengtson, M. Ordoñez, W. Vaca, A. Dhondt, J. Suárez, and J. Toro (2008), Sedimentary record of terminal Cretaceous accretions in Ecuador: The Yunguilla Group in the Cuenca area, *J. South Am. Earth Sci.*, 25, 133–144.
- Jaillard, E., H. Lapierre, M. Ordoñez, J. Toro, A. Amortegui, and J. Vanmelle (2009), Accreted oceanic terranes in Ecuador: Southern edge of the Caribbean Plate? *Geol. Soc. London Spec. Publ.*, 328, 469–485, doi:10.1144/SP328.19.

- Kawakatsu, H., and G. Proaño (1991), Focal mechanisms of the March 6, 1987 Ecuador earthquakes—CMT inversion with a first motion constraint, *J. Phys. Earth*, *39*, 589–597.
- Kellogg, J., and V. Vega (1995), Tectonic development of Panama, Costa Rica, and the Colombian Andes: Constraints from global positioning system geodetic studies and gravity, *Geol. Soc. Am. Spec. Pap.*, *295*, 75–90.
- Kerr, A., J. Aspden, J. Tarney, and L. Piltasig (2002), The nature and provenance of accreted oceanic terranes in western Ecuador: Geochemical and tectonic constraints, *J. Geol. Soc.*, *159*, 577–594.
- La Femina, P., T. H. Dixon, R. Govers, E. Norabuena, H. Turner, A. Saballos, G. Mattioli, M. Protti, and W. Strauch (2009), Fore-arc motion and Cocos Ridge collision in Central America, *Geochem. Geophys. Geosyst.*, *10*, Q05S14, doi:10.1029/2008GC002181.
- Lallemand, S. (1999), *La Subduction Océanique*, pp. 193, Gordon and Breach Science Publishers, Amsterdam.
- Lavenu, A., C. Noblet, M. G. Bonhomme, A. Eguez, F. Dugas, and G. Viver (1992), New K-Ar age dates of Neogene and Quaternary volcanic rocks from the Ecuadorian Andes: Implications for the relationship between sedimentation, volcanism, and tectonics, *J. South Am. Earth Sci.*, *5*(374), 309–320.
- Lavenu, A., T. Winter, and F. Dávila (1995), A Pliocene-Quaternary compressional basin in the Interandean Depression, Central Ecuador, *Geophys. J. Int.*, *121*, 279–300.
- Lebras, M., F. Mégard, C. Dupuy, and J. Dostal (1987), Geochemistry and tectonic setting of pre-collision Cretaceous and Paleogene volcanic rocks of Ecuador, *Geol. Soc. Am. Bull.*, *99*, 569–578.
- Legrand, D., P. Baby, F. Bondoux, C. Dorbath, S. Bès de Berc, and M. Rivadeneira (2005), The 1999–2000 seismic experiment of Macas swarm (Ecuador) in relation with rift inversion in Subandean foothills, *Tectonophysics*, *395*, 67–80.
- Lions, R. (1995), Evolution géodynamique d'un bassin d'avant-arc Néogène en contexte décrochant: L'ouverture du Golfe de Guayaquil, D.E. A., Université Joseph Fourier-Grenoble I, pp. 30.
- Luzieux, L. D. A., F. Heller, R. Spikings, C. Vallejo, and W. Winkler (2006), Origin and Cretaceous tectonic history of the coastal Ecuadorian forearc between 1°N and 3°S: Paleomagnetic, radiometric and fossil evidence, *Earth Planet. Sci. Lett.*, *249*, 400–414.
- Mamberti, M., H. Lapierre, D. Bosch, E. Jaillard, R. Ethien, J. Hernandez, and M. Polve (2003), Accreted fragments of the Late Cretaceous Caribbean-Colombian Plateau in Ecuador, *Lithos*, *66*, 173–199.
- Manchuel, K., M. Regnier, N. Bethoux, Y. Font, V. Sallares, J. Díaz, and H. Yepes (2011), New insights on the interseismic active deformation along the north Ecuadorian-south Colombian (NESC) margin, *Tectonics*, *30*, TC4003, doi:10.1029/2010TC002757.
- McCaffrey, R. (1992), Oblique plate convergence, slip vectors and forearc deformation, *J. Geophys. Res.*, *97*(B6), 8905–8915, doi:10.1029/92JB00483.
- Melnick, D., B. Bookhagen, M. R. Strecker, and H. P. Echtler (2009), Segmentation of megathrust rupture zones from forearc deformation patterns over hundreds to millions of years, Arauco peninsula, Chile, *J. Geophys. Res.*, *114*, B01407, doi:10.1029/2008JB005788.
- Mendoza, C., and J. Dewey (1984), Seismicity associated with the great Colombia-Ecuador earthquakes of 1942, 1958, and 1979: Implications for barrier models of earthquake rupture, *Bull. Seismol. Soc. Am.*, *74*(2), 577–593.
- Molnar, P., and K. Dayem (2010), Major intracontinental strike-slip faults and contrasts in lithospheric strength, *Geosphere*, *6*(4), 444–467, doi:10.1130/GES00519.1.
- Mothes, P. A., J.-M. Nocquet, and P. Jarrín (2013), Continuous GPS network operating throughout Ecuador, *Eos Trans. AGU*, *94*(26), 229.
- Naesser, C., J. Crochet, E. Jaillard, G. Laubacher, T. Mourier, and B. Sige (1991), Tertiary fission-track ages from the Bagua syncline (northern Peru): Stratigraphic and tectonic implications, *J. South Am. Earth Sci.*, *4*(1/2), 61–71.
- Nocquet, J.-M., et al. (2014), Motion of continental slivers and creeping subduction in the northern Andes, *Nat. Geosci.*, doi:10.1038/ngeo2099.
- Paris, G., M. Machette, R. Dart, and K. Haller (2000), Map and database of Quaternary faults and folds in Colombia and its offshore regions, A project of the International Lithosphere Program Task Group II-2, Major Active Faults of the World, Open-File Report 00-0284 USGS.
- Pennington, W. (1981), Subduction of the Eastern Panama Basin and seismotectonics of northwestern South America, *J. Geophys. Res.*, *86*(B11), 10,753–10,770, doi:10.1029/JB086iB11p10753.
- Pindell, J., and L. Kennan (2009), Tectonic evolution of the Gulf of Mexico, Caribbean and northern South America in the mantle reference frame: An update, *Geol. Soc. London Spec. Publ.*, *328*, 1–55, doi:10.1144/SP328.1.
- PMA: GCA Programa Multinacional Andino Geociencia para las Comunidades Andinas; Canada y Sud América (2009), Atlas de deformaciones cuaternarias de los Andes: Review articles/Book and Digital Maps available in Geological Surveys in South America Publicacion Geológica Multinacional, No. 7, 320, 1 mapa en CD-ROM. [Available at [http://can.geosemantica.net/collections/documents\\_folderview.aspx?c=1](http://can.geosemantica.net/collections/documents_folderview.aspx?c=1), Or neotec-opendata.com.]
- Pratt, W., P. Duque, and M. Ponce (2005), An autochthonous geological model for the eastern Andes of Ecuador, *Tectonophysics*, *399*, 251–278.
- Reynaud, C., E. Jaillard, H. Lapierre, M. Mamberti, and G. Masclé (1999), Oceanic plateau and island arcs of southwestern Ecuador: Their place in the geodynamic evolution of northwestern South America, *Tectonophysics*, *307*, 235–254.
- Ruiz, G. M. H. (2002), Exhumation of the northern Sub-Andean Zone of Ecuador and its source regions: A combined thermochronological and heavy mineral approach. PhD, ETH-Zürich, Switzerland.
- Segovia, M., and A. Alvarado (2009), Breve análisis de la sismicidad y del campo de esfuerzos en el Ecuador, in *Geología y Geofísica Marina y Terrestre del Ecuador: Desde la Costa Continental Hasta las Islas Galápagos*, edited by J.-Y. Collot, V. Sallares, and N. Pazmiño, pp. 131–150, Comisión Nacional del Derecho del Mar (CNDM) — Institut de Recherche pour le Développement (IRD) — Instituto Oceanográfico de la Armada (INOCAR), Guayaquil, Ecuador.
- Soulas, J.-P., A. Eguez, H. Yepes, and V. H. Pérez (1991), Tectónica activa y riesgo sísmico en los Andes Ecuatorianos y el extremo Sur de Colombia, *Bol. Geol. Ecuatoriano*, *2*, 3–11.
- Souris, M. (2003), L'Equateur en 28 millions de points, Sciences Au Sud n°21, Paris.
- Spikings, R., and P. Crowhurst (2004), (U-Th)/He thermochronometric constraints on the late Miocene-Pliocene tectonic development of the northern Cordillera Real and the Interandean Depression, Ecuador, *J. South Am. Sci.*, *17*, 239–251.
- Spikings, R., D. Seward, W. Winkler, and G. Ruiz (2000), Low-temperature thermochronology of the northern Cordillera Real, Ecuador: Tectonic insights from zircon and apatite fission track analysis, *Tectonics*, *19*(4), 619–668, doi:10.1029/2000TC900010.
- Spikings, R., W. Winkler, D. Seward, and R. Handler (2001), Along-strike variations in the thermal and tectonic response of the continental Ecuadorian Andes to the collision with heterogeneous oceanic crust, *Earth Planet. Sci. Lett.*, *186*, 57–73.
- Spikings, R., W. Winkler, R. Hughes, and R. Handler (2005), Thermochronology of allochthonous terranes in Ecuador: Unravelling the accretionary and post-accretionary history of the Northern Andes, *Tectonophysics*, *399*, 195–220.
- Spikings, R., P. Crowhurst, W. Winkler, and D. Villagomez (2010), Syn- and post-accretionary cooling history of the Ecuadorian Andes constrained by their in-situ and detrital thermochronometric record, *J. South Am. Sci.*, *30*, 121–133.
- Steinmann, M., D. Hungerbühler, D. Seward, and W. Winkler (1999), Neogene tectonic evolution and exhumation of the southern Ecuadorian Andes: A combined stratigraphy and fission-track approach, *Tectonophysics*, *307*, 255–276.

- Suarez, G., P. Molnar, and B. C. Burchfiel (1983), Seismicity, fault plane solutions, depth of faulting, and active tectonics of the Andes of Peru, Ecuador, and Southern Colombia, *J. Geophys. Res.*, *88*(B12), 10,403–10,428, doi:10.1029/JB088iB12p10403.
- Tapponnier, P., and P. Molnar (1979), Active faulting and Cenozoic tectonics of the Tien Shan, Mongolia, and Baykal Regions, *J. Geophys. Res.*, *84*(B7), 3425–3459, doi:10.1029/JB084iB07p03425.
- Tapponnier, P., X. Zhiqin, F. Roger, B. Meyer, N. Arnaud, G. Wittlinger, and Y. Jingsui (2001), Oblique stepwise rise and growth of the Tibet Plateau, *Science*, *294*(5547), 1671–1677.
- Tibaldi, A., and L. Ferrari (1992), Latest Pleistocene-Holocene tectonics of the Ecuadorian Andes, *Tectonophysics*, *205*, 109–125.
- Tibaldi, A., A. Rovida, and C. Corazzato (2007), Late Quaternary kinematics, slip-rate and segmentation of a major Cordillera-parallel trans-current fault: The Cayambe-Afiladores-Sibundoy system, NW South America, *J. Struct. Geol.*, *29*, 664–680.
- Toro, J. (2007), Enregistrement des surrections liées aux accrétions de terrains océaniques: Les sédiments Crétacé-Paléogènes des Andes d'Equateur, *Géologie Alpine, Mémoire H.S. No 47*, Université Joseph Fourier (Grenoble I) France, pp. 235.
- Troncoso, L. (2009), Estudio sismológico del Nido de Pisayambo, Master 2, Université Sophia-Antipolis (Nice) France, pp 26.
- Uyeda, S., and H. Kanamori (1979), Back-arc opening and the mode of subduction, *J. Geophys. Res.*, *84*(B3), 1049–1061, doi:10.1029/JB084iB03p01049.
- Van Thournout, F., J. Hertogen, and L. Quevedo (1992), Allochthonous terranes in northwestern Ecuador, *Tectonophysics*, *205*(1-3), 205–22.
- Velandia, F., J. Acosta, R. Terraza, and H. Villegas (2005), The current tectonic motion of the Northern Andes along the Algeciras fault system in SW Colombia, *Tectonophysics*, *399*, 313–329.
- Wang, K., Y. Hu, M. Bevis, E. Kendrick, R. Smalley, R. B. Vargas, and E. Lauría (2007), Crustal motion in the zone of the 1960 Chile earthquake: Detangling earthquake-cycle deformation and forearc-sliver translation, *Geochem. Geophys. Geosyst.*, *8*, Q10010, doi:10.1029/2007GC001721.
- White, S., R. Trenkamp, and J. Kellogg (2003), Recent crustal deformation and the earthquake cycle along the Ecuador-Colombia subduction zone, *Earth Planet. Sci. Lett.*, *216*, 231–242, doi:10.1016/S0012-821X(03)00535-1.
- Winkler, W., D. Villagómez, R. Spikings, P. Abegglen, S. Tobler, and A. Egüez (2005), The Chota basin and its significance for the inception and tectonic setting of the inter-Andean depression in Ecuador, *J. South Am. Earth Sci.*, *19*, 5–10.
- Winter, T., J.-P. Avouac, and A. Lavenu (1993), Late Quaternary kinematics of the Pallatanga strike-slip fault (Central Ecuador) from topographic measurements of displaced morphological features, *Geophys. J. Int.*, *115*, 905–920.
- Witt, C., and J. Bourgois (2010), Forearc basin formation in the tectonic wake of a collision-driven, coastwise migrating crustal block: The example of the North Andean Sliver and the extensional Gulf of Guayaquil-Tumbes Basin (Ecuador-Perú border area), *GSA Bull.*, *122*, 89–108, doi:10.1130/B26386.1.
- Witt, C., J. Bourgois, F. Michaud, M. Ordoñez, N. Jiménez, and M. Sosson (2006), Development of the Gulf of Guayaquil (Ecuador) during the Quaternary as an effect of the North Andean block tectonic escape, *Tectonics*, *25*, TC3017, doi:10.1029/2004TC001723.
- Zamora, A., and M. Litherland (1993), Mapa Geológico de la República del Ecuador, escala 1: 1.000.000. Corporación de Desarrollo e Investigación Geológico Minero-Metalúrgica y Misión Geológica Británica-British Geological Survey, Ministerio de Energía y Minas, Quito-Ecuador.